Tesi doctoral presentada per En/Na

Laura VILLANUEVA ÁLVAREZ

amb el títol

"Ecophysiological and molecular characterization of estuarine microbial mats"

per a l'obtenció del títol de Doctor/a en

BIOLOGIA

Barcelona, 22 de desembre de 2005.

Facultat de Biologia
Departament de Microbiologia

UNIVERSITAT DE BARCELONA

V. REDOX STATE AND COMMUNITY COMPOSITION IN MICROBIAL MATS FROM DIFFERENT LOCATIONS
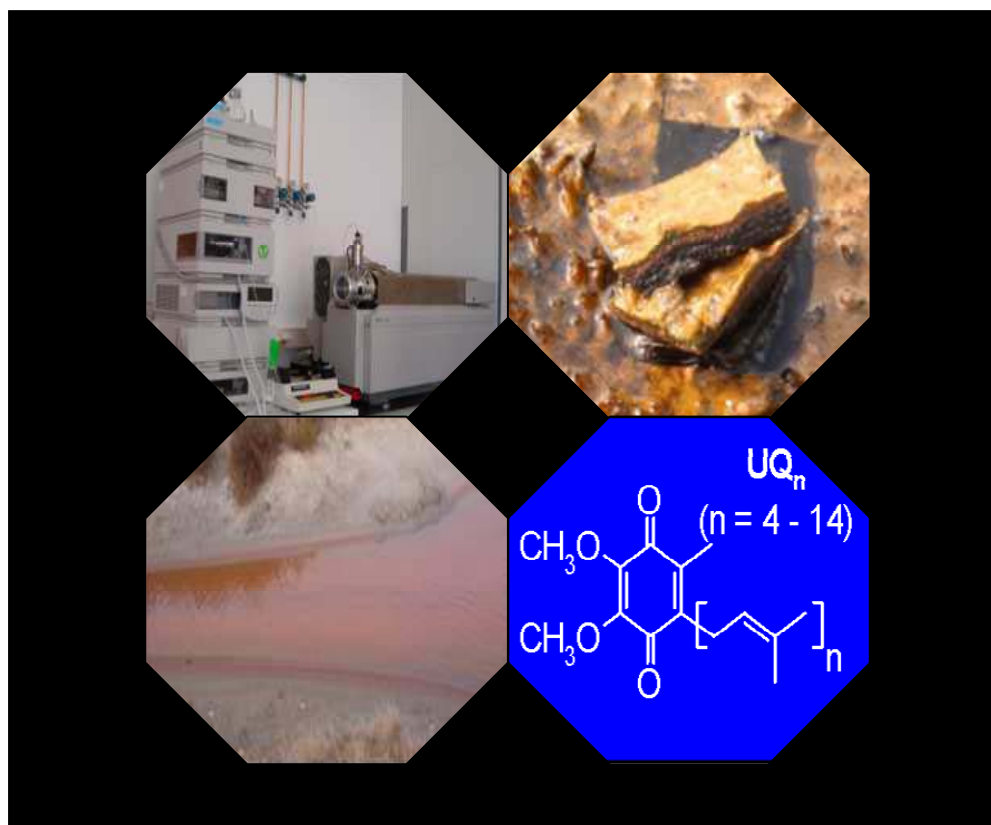

Figure V. "True science teaches, above all, to doubt and to be ignorant" Miguel de Unamuno (1864–1936).

From top left to right: Liquid chromatography tandem mass spectrometry Applied Biosystems/MDS Sciex 4000 QTrap™ / Ebro Delta microbial mat / Halophilic pond of a solar saltern in 'Les Salines de la Trinitat' / Ebro Delta (Spain) / Ubiquinone structure.

- Introduction and objectives of the study

In general, microbial mats from different locations develop comparable steep gradients of physiochemical conditions forming highly structured environments. In such environment, relevant functional microbial groups establish strong interactions and form 'microniches'. The study of the enormous microbial diversity of this kind of ecosystems improves the understanding of biochemical cycles and of reasons why apparently similar structured systems reveal differential characteristics.

Lipid biomarkers have been considered as effective markers of microbial community structure (see 'I. Introduction', 'Lipid biomarkers and the SLB approach' section). Several studies have demonstrated that the relative abundance and vertical distribution of lipid components indicate the spatial and trophic structure of the mat community (Ward *et al*., 1989; Zeng *et al*., 1992). As it has been mentioned in the 'Introduction' chapter, these lipid components are not always fatty acid methyl esters, since many other lipid classes can be used as unique markers of microbial groups.

The analysis of microbial quinones has gained increased recognition as a simple and useful approach for studying microbial structure in environmental samples (Hiraishi, 1988; Fujie *et al*., 1998; Hu *et al*., 1999 and 2001). In fact, the isoprenoid quinones are taxonomic tools due to their structural variation in different taxonomic groups (Collins and Jones, 1981), and they are specific biomarkers of microbial metabolism (Hedrick and White, 1986). Another interesting issue of the quinone profiling method is the use of indices that estimate the differences in quinone profiles quantitatively and allow the processing of data by statistical methods (Hiraishi, 1999).

The community composition of microbial mats has been assessed by PLFA (phospholipid fatty acid) content in several studies (Ward *et al*., 1989; Navarrete *et al*., 2000, 2004). However, the major fatty acids recovered from mat systems ('IV. Vertical microscale characterization of bacterial diversity and physiological status' chapter) are often very common and thus are not all diagnostic. Therefore, the study of intact polar lipids has been proposed to improve the identification of sources of the major mat lipids (Ward *et al*., 1994).

Intact polar lipids (IPLs) are attractive analytical targets because they are taxonomically more specific than their apolar derivatives and avoid exclusion of signals from prokaryotes that primarily build their membranes with ether-bound lipids such as *Archaea* and some bacteria. Almost all studies on the molecular structures of archaebacterial ether lipids have involved hydrolysis of the polar head groups from the intact lipid and selective cleavage of ether linkages (Sprott, 1992; Gattinger *et al.*, 2003). However, the similar structural features of ether lipid core structures have made this kind of analysis very difficult and the analysis as intact lipids is a promising alternative (Qiu *et al.*, 2000; Sturt *et al.*, 2004).

Archaea represent a considerable fraction of the prokaryotic world in marine and terrestrial ecosystems, indicating that organisms from this domain might have a large impact on global energy cycles. *Archaea* domain is divided into four phyla, *Euryarchaeota*, *Crenarchaeota*, *Korarchaeota*, the presence of which has been determined only by environmental DNA sequences (Barns *et al.*, 1996; Bano *et al.*, 2004), and the recently reported *Nanoarchaeota* (Huber *et al.*, 2002). Several recent molecular studies (Jurgens *et al.*, 1997; Buckley *et al.*, 1998) have demonstrated the ubiquity of *Archaea* in soil, particularly those organisms belonging to the non-thermophilic *Crenarchaeota* lineage. Archaeal members have been detected in microbial mats from different locations (Brambilla *et al.*, 2001; Ramirez-Moreno *et al.*, 2003; Rothrock and García-Pichel, 2005; Blumenberg *et al.*, 2005). However, the affiliations and physiology of these members are still unknown.

The aim of this study was (i) the determination of how depth-related changes and site differences affect the quinone composition in certain microbial mats, (ii) the identification of intact polar lipids from specific microbial groups in mats by LC/MS/MS, and (iii) cloning and sequencing of archaeal 16S rDNA fragments from microbial mats and establishing relationships with the data obtained by the intact lipid and quinone profiling methods.

- ## Material and methods

> ### Sampling and preparation of the samples

Ebro delta, halophilic pond, and Camargue microbial mats were sampled in November 2004 at 12:00 GMT. The halophilic pond was a cristallizer saltern located in 'Les Salines de la Trinitat' Ebro Delta (Spain) integrated in a semi-artificial coastal system designated to harvest common salt from sea water. Mat samples for quinone and intact lipid analysis were collected as cores removed from the upper part of the mat with a cork borer. Samples used for depth analyses, were sectioned (50 µm) in a cryomicrotome. Combining adjacent slides, 500-µm-thick horizontal mat sections were obtained and prepared as was described in chapter 'Material and methods'. The total depth analyzed for Ebro delta and Camargue mat samples was 7.75 mm.

> ### Analysis of isoprenoid quinones

Total lipid was obtained from the Ebro delta and Camargue sectioned samples, Ebro delta mat as a 'whole-core', and the 'halophilic pond' samples. The total lipids extracts were separated by silicic acid choromatography as described in the section '2. Lipid analysis methods' ('II. General Material and Methods'). The obtained neutral lipid fraction was analyzed for the identification and quantification of isoprenoid quinones ('Neutral lipid fraction analysis', 'II. General Material and Methods').

The numerical analysis was performed by using the Microsoft® Office Excel facility. Three different parameters were calculated: the microbial divergence index of ubiquinones and menaquinones (*MD* ub+mk), the bioenergetic divergence index (*BD* ub+mk), and the divergence index (*D*) (Iwasaki and Hiraishi, 1998; Hiraishi, 1999). *MD* ub+mk values represent the divergence of ubiquinone and menaquinone structural types detected and it can be used as an indicator of microbial diversity. *MD* ub+mk is calculated according to Eq1:

$$MD\text{q} = \left(\sum_{k=1}^{n} \sqrt{X_k} \right)^2 \quad [1]$$

where $X_k \geq 0.001$ and X_k indicates the molar ratio of the content of the quinone homolog k to the total quinone content.

BDq is regarded as an indicator of the divergence of bioenergetic modes of microorganisms and calculated as BD ub+mk by Eq2:

$$BD \text{ ub+mk} = \left(\sqrt{UQ} + \sqrt{MK} \right)^2 \quad [2]$$

where UQ (ubiquinone), and MK (menaquinone) ≥ 0.001, and indicate the molar fractions of UQ, MK and their derivatives, compared to the total quinone content. In this case BD ub+mk indicates the balance of ubiquinone-mediated aerobic respiration, and menaquinone-mediated anaerobic and aerobic respiration. The divergence index (D) can be interpreted to reveal the extent of differences in microbial community structures among samples. D is calculated by Eq3:

$$D(i,j) = \frac{1}{2} \sum_{k=1}^{n} |X_{ki} - Xkj| \quad [3]$$

where $X_{ki}, X_{kj} \geq 0.01$, $\Sigma X_{ki} = \Sigma X_{kj} = 100$, and X_{ki} and X_{kj} indicate the levels (expressed as percent of moles) of the quinone homolog k in samples i and j, respectively. The neighbor-joining algorithm (Saitou and Nei, 1987) was used to construct a dendrogram based on D matrix data using the Mega 3.0 software. In this study, ubiquinones, menaquinones, demethylmenaquinones, and plastoquinones with n isoprene units in their side chain were abbreviated as Q-n, MK-n, DMK-n and PQ-n, respectively. Phylloquinone (vitamin K_1) was abbreviated as K_1. Reproducibility of quinone analysis was within $\pm$ 5% (data obtained from $n = 4$ replicates of microbial mat sample cores obtained at the same sampling time). The value %mol was defined as picomoles (pmol) of certain quinone homolog in a sample divided by the picomole sum of all measured quinones set to 100% in that sample.

➢ Intact polar lipid analysis

After the silicic acid chromatography of the total lipid extracts, the polar lipid fraction was analyzed, without further treatment, by LC/MS/MS in order to identify and quantify intact polar lipids ('Intact polar lipid analysis', 'II. Material and Methods').

➢ PCR, cloning and sequencing of 16S rDNA sequences from *Archaea*

Ebro Delta and Camargue mat samples, as a 'whole-lyophilized core', were homogenized and 0.15 g of each sample were used to perform a DNA extraction with the Power Soil™ DNA isolation kit (Mo Bio Laboratoires, Inc.). *Archaea*-specific primers ARQ21F and ARQ958R were used to amplify a 16S rDNA fragment as was described in Table II.5 and II.6 of the 'General Material and Methods' chapter. The PCR products were purified with the Wizard® PCR Preps (Promega) kit and then cloned using the pGEM® T vector system. Positive clones were isolated as a pure culture and some colonies were boiled and the aqueous supernatant was used as a template in a PCR reaction with the pGEM-T vector primers (see Table II.5 and II.6). The PCR reaction products of the cloned insert were precipitated and digested to check the presence of different cloned bands by digestion patterns (*EcoR*I+*Hind*III and *Sma*I). Sequences that were of high frequency in clone libraries were selected for sequence analysis (see Table II.8, 'II. General Material and Methods').

The occurrence of chimeras was checked by using the Chimera_check program (see 'Bioinformatic and phylogenetic analyses' section of 'II. General Material and Methods'), and the obtained sequences were aligned with Genbank-downloaded sequences. Evolutionary distance trees (Neighbor-joining algorithm, Jukes and Cantor correction) were constructing by using Mega 3.0 software.

- Results

  ➢ <u>Quinone profiles</u>

Structural variations exhibited by quinone isoprenologues types can be used as criteria for the classification of microorganisms at taxonomic level. This fact allows the observation of composition and variation of certain bacterial groups in environmental samples (Collins and Jones, 1981). Quinone composition and changes in their profile with depth are summarized in Fig. V.1 and V.2 for Ebro delta and Camargue microbial mats. Likewise, quinone composition as %mol for Ebro delta mat sample ('all-core') and the 'halophilic pond' sample are shown in Fig. V.3.

An important variety of quinone homologues was detected at all sampling sites and depths examined. Ebro delta microbial mat profile was characterized by a higher abundance of Q-8 (from 22.26% in the upper layers to a maximum of 54.7% in 2.5–3 mm) at all depths except from 0–1.5 mm depth where Q-10 was the major quinone. Indeed, the relative percentage of Q-10 decreased in the middle layers in comparison with the values detected from 0–2 mm and 5–7.75. Q-9 was also important from 0–1.5 mm and then, its %mol decreased remaining at the same level at all depths. Q-6 was the less representative ubiquinone, and also among the total quinones as well as DMKs, in all the vertical profile. Based on chemotaxonomic studies, β- and γ-Proteobacteria, γ-Proteobacteria, and α-Proteobacteria, were considered as possible major sources of Q-8, Q-9 and Q-10, respectively.

A clear dominance was not detected among menaquinones. However, in all Ebro delta samples short chain menaquinones (MK-6, 7, 8) were the most abundant menaquinone homologues except from 4–5.5 mm depth in where MK-9 reported the highest percentage among MKs. MK-6 was the most abundant at the top of the mat (0–1 mm) as well as MK-7 that showed a high %mol from 2–4 mm and at the deepest layers together with MK-8. As possible sources of MK-6 and MK-7 are considered members of the *Cytophaga-Flavobacterium* group, ε-Proteobacteria (MK-6), and δ-Proteobacteria (probably sulfate-reducing bacteria). *Firmicutes* and members of the *Archaea* phylum (also source of MK-7) have been reported to contribute to the MK-8 pool. The %mol of

MK-10 was higher from 0–2.5 mm and then decreased with depth; however, its presence was reported at all depths. Their possible sources are green non-sulfur bacteria and *Actinobacteria*.

In comparison with Ebro delta mats, Camargue mat samples did not show a quinone homolog dominant in all depths (Fig. V.2). So, MK-9 was dominant from 0–4 mm and then Q-8 showed the highest percentage from 4–7.75 mm. As possible sources of MK-9 are *Firmicutes*, *Actinobacteria* and the *Bacteroides* group. In addition, the percentage of MK-7 was higher from 3–7.75 mm, as well as MK-8. MK-4 was the least representative among menaquinones, and MK-10 showed higher percentages from 0 to 4 mm than at the layers. Below, demethylmenaquinones 8 and 9 were detected at a very low %mol in all samples, especially DMK-9 that was not observed in Camargue samples. Indeed, demethylmenaquinone sources have been only reported in certain genus of the *Enterobacteriales* and *Aeromonadales* order (Whistance and Threlfall, 1968; Collins and Jones, 1981).

In the 'halophilic pond' sample, a lower variety of quinone homologues were identified compared to microbial mat samples (Fig. V.3). The quinones, Q-6, 7, 10 and MK-9 were not found in that sample. MK-8 was the major component (27.55%) but a high %mol of MK-10 and 4 were also detected (18.79 and 13.89%, respectively), as well as MK-5, 6 and 7. Among the ubiquinones only Q-8 (γ and β-Proteobacteria) and Q-9 (γ-Proteobacteria) were detected in that sample. In the Ebro delta 'all-core' sample the dominant quinone were Q-8 (27.15%) and also MK-9 (25.18%). Likewise, MK-7 and M-8 (*Firmicutes*, *Cytophaga-Flavobacterium*, δ-Proteobacterium, *Actinobacteria* and *Archaea*) contributed to a significant percentage.
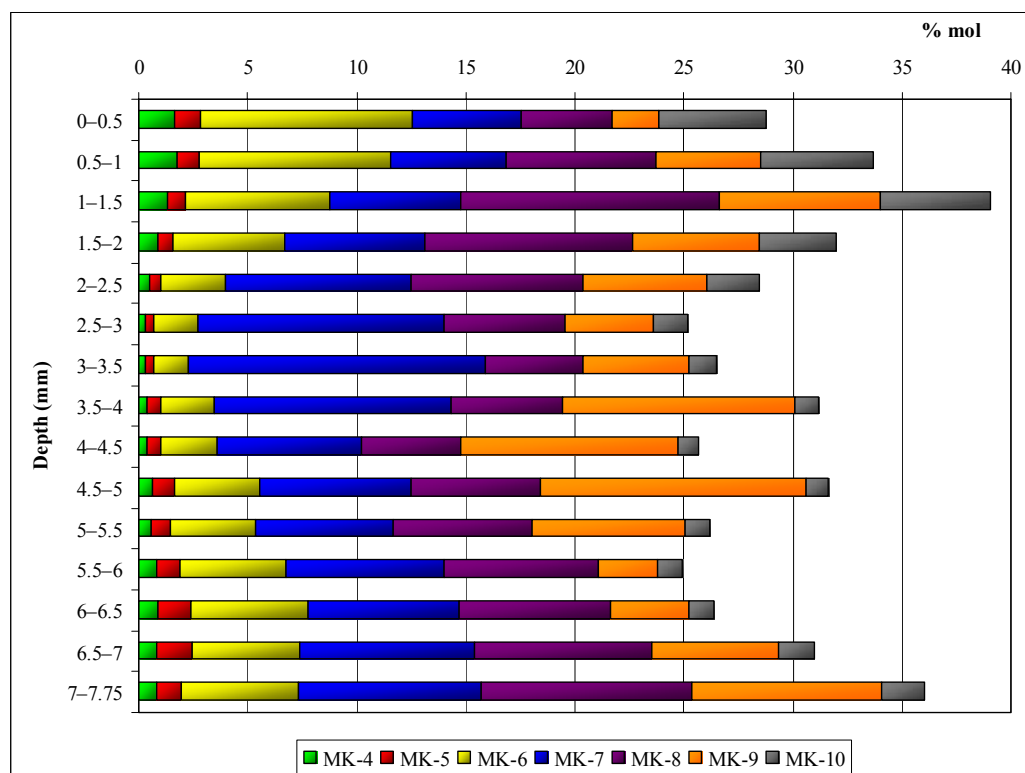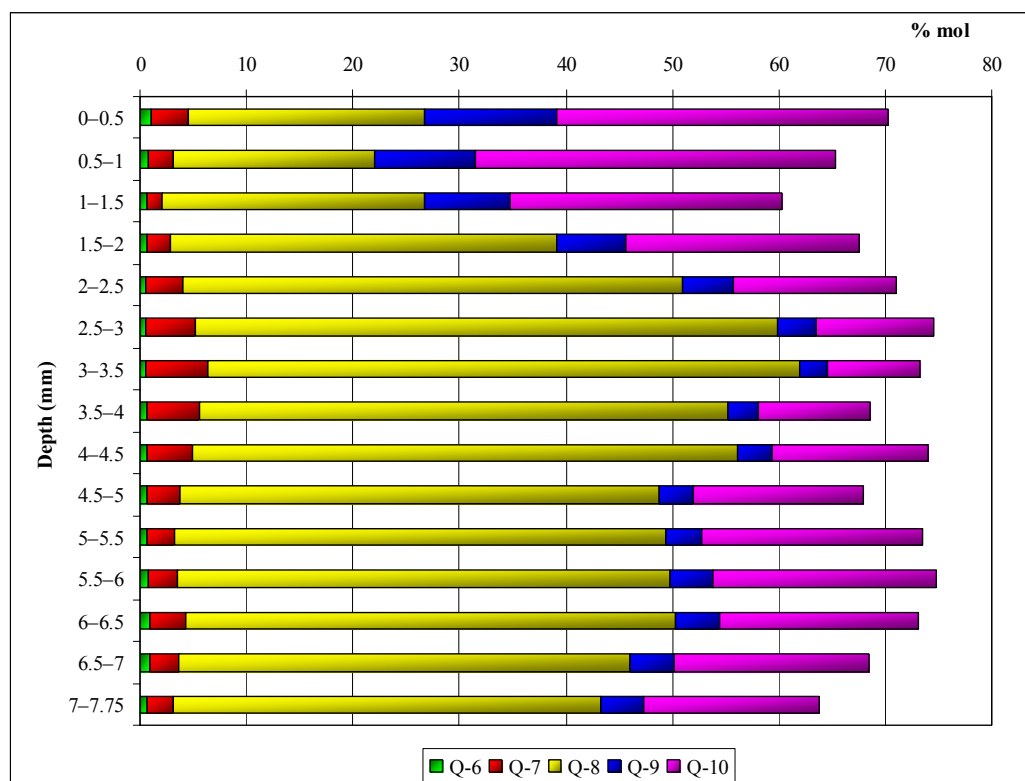
Figure V.1. Ubiquinone (Q) and menaquinone (MK) composition of Ebro delta mat samples.

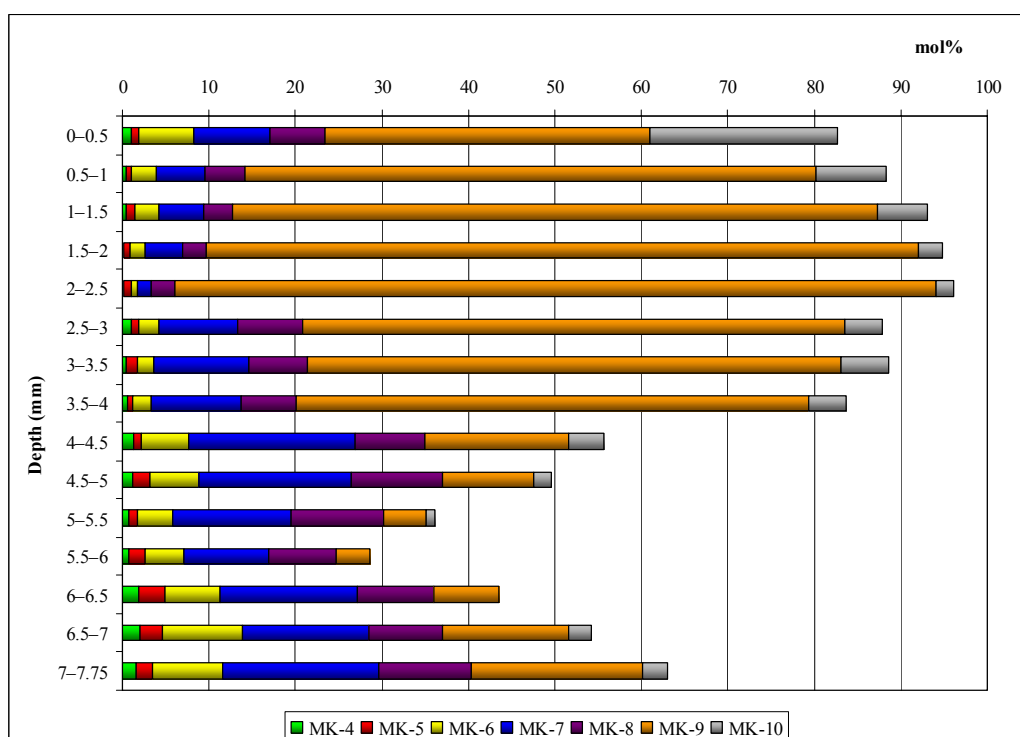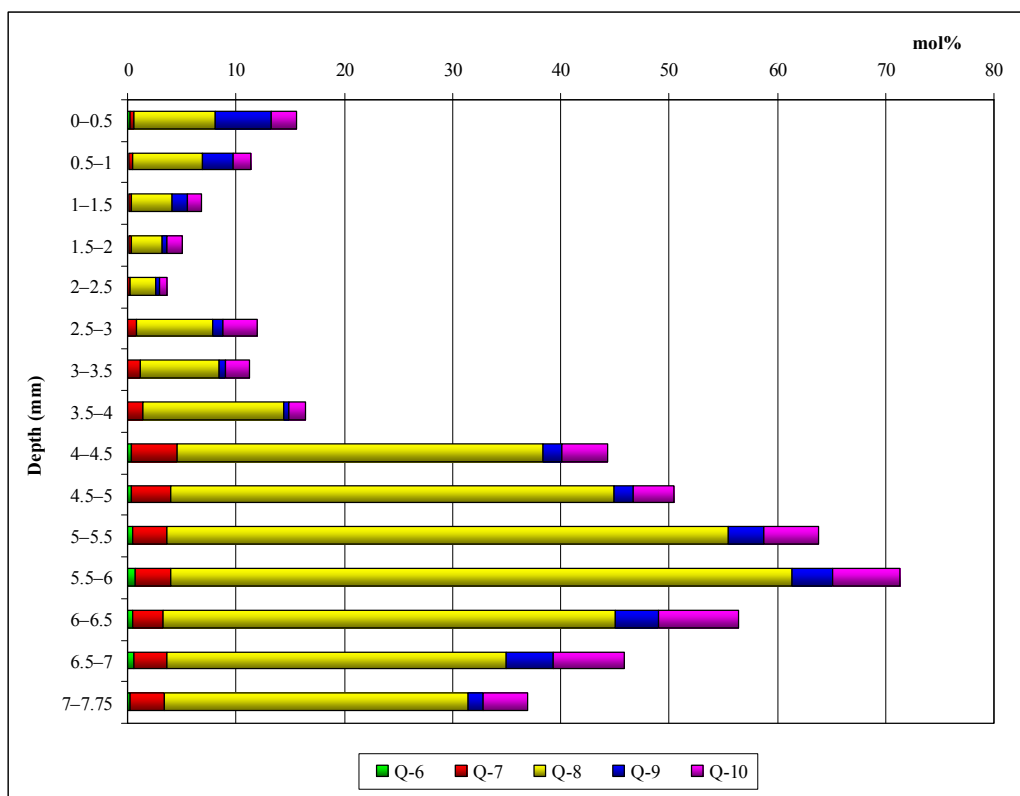Quinone content is given as %mol. Reproducibility of quinone analysis was within ±5%.

Figure V.2. Ubiquinone (Q) and menaquinone (MK) composition of Camargue mat samples.

Quinone content is given as %mol. Reproducibility of quinone analysis was within ±5%.
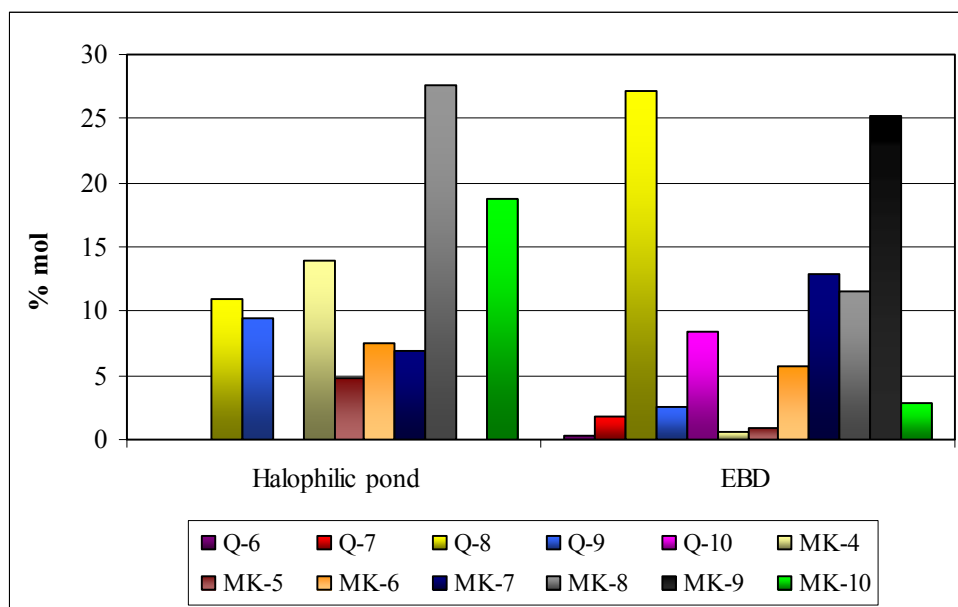
Figure V.3. Quinone composition of the 'Halophilic pond' and 'Ebro delta all-core' (EBD) samples.

In order to give an idea about the amount of quinones in each samples, the percentages of certain quinones (pmol g^{-1} dry weight regarding the total quinone content as pmol g^{-1} dry weight) are summarized in Table V.1 and V.2. Considerable amounts of photosynthetic quinones, plastoquinone-9 (PQ-9) and phylloquinone (K_1), were detected in both mat systems, especially in Camargue microbial mats with a maximum of 5.8×10^4 pmol K_1+PQ-9 g^{-1} dry weight at 1–1.5 mm depth. Ebro delta mat samples reported a lower content of photosynthetic quinones with a maximum one order of magnitude lower than in Camargue samples (6.5×10^3 pmol K_1+PQ-9 g^{-1} dry weight at the same depth). In Ebro delta mat samples the highest percentage of photosynthetic biomass, % ph-B (pmol g^{-1} dry weight of K_1+PQ-9 by total quinone content) was 25.8% at 1–1.5 mm depth; however, the highest percentage in Camargue vertical profile was found at 0–0.5 mm (83%). Both Ebro delta and Camargue samples revealed comparable vertical profiles of quinone content (Fig. V.4). A progressive increase started at the top of the mat with a maximum at 1–1.5 mm, then the abundance decreased until an inflexion point (at 6–6.5 mm for Camargue, and at 6.5–7 mm for Ebro delta) from where the photosynthetic quinones (PQ-9 and K_1) increased again.

238

The comparison between the amount of the main quinones in Ebro delta and Camargue mats revealed that the more abundant quinone in Ebro delta samples was Q-8 (3–3.5 mm), and K_1 in Camargue mats at all depths except for 5–6 mm where Q-8 was higher. Moreover, the amount of MK-9 was higher at the top of the mat (0.5–4 mm) in comparison with Ebro delta samples that reported higher values from 3–5.5 mm. In both mats, MK-10 had higher values at the top of the mat. Besides, Q-10 indicative of α-Proteobacteria was low in Camargue mats; however, Ebro delta mat reported important values of this quinone throughout the vertical profile. Additionally, the relative abundance of K_1 was greater than that of PQ-9 in all samples, and PQ-9 was only detected in Camargue mats. Moreover, the highest percentage of the total quinone content in the 'halophilic pond' sample was detected for MK-8 (27.5%), and K_1 (40.6%) in the 'Ebro delta all-core' sample. In the 'Ebro delta all-core' sample, PQ-9 was detected (9.7%) and Q-8 and MK-9 reported a similar percentage (Table V.3).

Table V.1. Percentages of certain quinones in relation to the total quinone content (calculated from picomoles per gram of dry weight in Ebro delta mat samples).

Depth (mm)	Q-8	Q-10	MK-6	MK-7	MK-8	MK-9	MK-10	% ph-B[1]	TQ[2] pmol g^{-1}
0–0.5	19.47	27.27	8.51	4.32	3.64	1.89	4.30	12.54	5873.16
0.5–1	14.06	25.29	6.54	3.92	5.14	3.59	3.88	25.42	10626.27
1–1.5	18.22	18.97	4.90	4.46	8.82	5.45	3.77	25.80	25096.31
1.5–2	28.13	16.98	3.96	5.01	7.36	4.51	2.70	22.55	25752.68
2–2.5	38.69	12.69	2.46	6.98	6.51	4.66	2.01	17.59	29244.96
2.5–3	50.08	10.09	1.83	10.37	5.06	3.72	1.44	8.44	51234.18
3–3.5	51.93	8.14	1.50	12.72	4.18	4.55	1.22	6.48	37192.03
3.5–4	47.08	9.95	2.31	10.28	4.85	10.10	1.03	5.34	21189.59
4–4.5	51.21	14.64	2.58	6.66	4.56	9.93	0.97	0.00	9118.70
4.5–5	44.95	16.04	3.94	6.91	5.94	12.19	1.01	0.00	4806.45
5–5.5	46.15	20.77	3.93	6.29	6.36	7.06	1.09	0.00	6734.55
5.5–6	46.31	20.92	4.88	7.28	7.04	2.73	1.10	0.00	7140.38
6–6.5	45.99	18.75	5.35	6.93	6.93	3.64	1.15	0.00	2942.11
6.5–7	42.41	18.34	4.91	8.05	8.12	5.80	1.66	0.00	1926.09
7–7.75	38.77	15.89	5.11	8.09	9.31	8.39	1.87	3.68	3579.23

[1](% ph-B) = percentage of photosynthetic biomass (PQ-n + K_1); [2]TQ = Total quinones.

Table V.2. Percentages of certain quinones in relation to the total quinone content (calculated from picomoles per gram of dry weight in Camargue mat samples).

Depth (mm)	Q-8	Q-10	MK-6	MK-7	MK-8	MK-9	MK-10	% ph-B[1]	TQ[2] pmol g^{-1}
0–0.5	1.22	0.36	1.02	1.41	1.03	6.01	3.50	83.94	43676.43
0.5–1	1.83	0.48	0.83	1.60	1.31	18.75	2.30	71.64	58376.55
1–1.5	1.18	0.39	0.84	1.62	1.05	23.03	1.75	69.12	83785.21
1.5–2	1.55	0.78	0.93	2.42	1.56	45.81	1.53	44.34	86745.98
2–2.5	1.66	0.53	0.53	1.13	1.98	62.92	1.42	28.53	75839.22
2.5–3	2.38	1.08	0.79	3.14	2.54	21.43	1.47	65.87	26796.27
3–3.5	2.77	0.86	0.71	4.20	2.56	23.38	2.10	62.10	35229.83
3.5–4	4.44	0.49	0.74	3.56	2.17	20.29	1.49	65.74	20259.16
4–4.5	11.08	1.40	1.81	6.29	2.68	5.46	1.32	67.17	12568.78
4.5–5	18.00	1.64	2.52	7.74	4.62	4.67	0.86	56.02	9981.48
5–5.5	34.55	3.36	2.63	9.21	7.13	3.22	0.72	33.30	10267.62
5.5–6	37.81	4.09	2.98	6.46	5.14	2.60	0.00	34.07	3375.97
6–6.5	23.12	4.14	3.46	8.83	4.87	4.22	0.00	44.58	2960.28
6.5–7	13.76	2.88	4.09	6.38	3.73	6.42	1.15	56.06	7716.88
7–7.75	9.89	1.47	2.84	6.40	3.78	7.04	1.00	64.62	8607.02

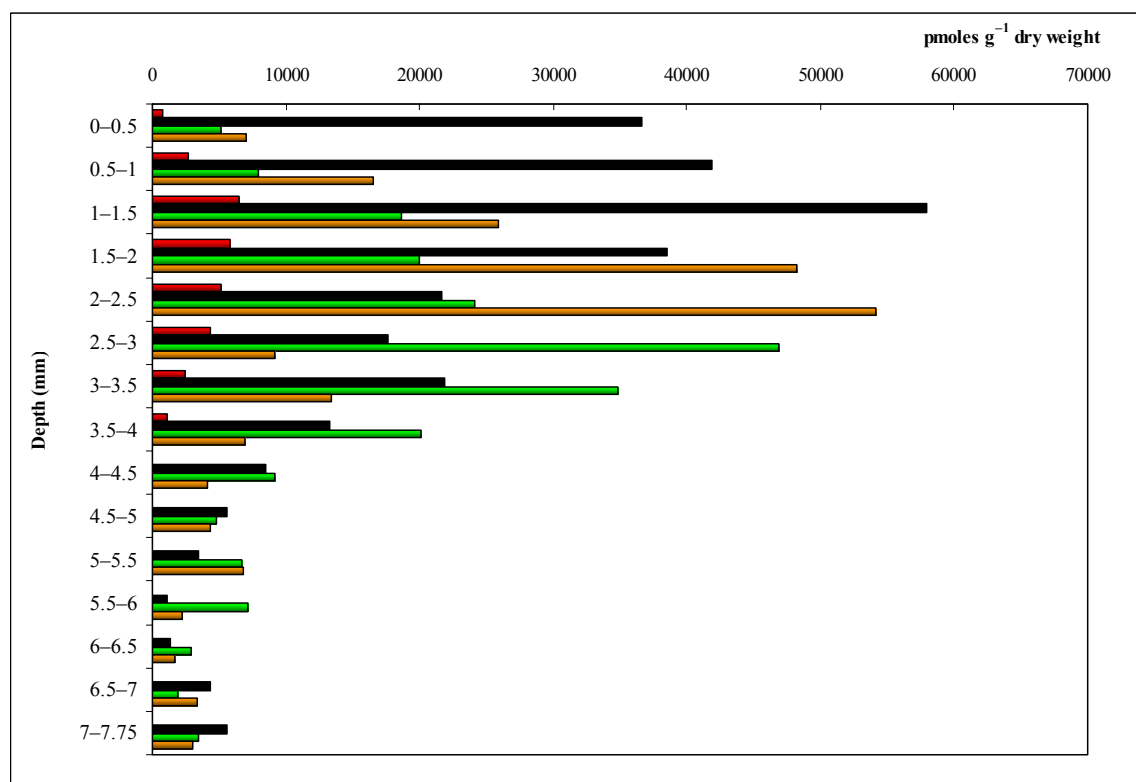[1](% ph-B) = percentage of photosynthetic biomass (PQ-n + K$_1$); [2]TQ = Total quinones.

Figure V.4. Quinone content as picomoles per gram of dry weight. (red Ebro mats photosynthetic quinones; black Camargue mats photosynthetic quinones; green Ebro mats non-photosynthetic quinones ub+mk+dmk; orange Camargue mats non-photosynthetic quinones).

Table V.3. Percentages of certain quinones in relation to the total quinone content (calculated from picomoles per gram of dry weight) in the 'Halophilic pond' and 'Ebro delta all-core' samples.

Homolog	Halophilic pond	EBD all-core	Homolog	Halophilic pond	EBD all-core
Q-6	0.00	0.17	MK-7	6.92	6.44
Q-7	0.00	0.91	MK-8	27.55	5.72
Q-8	11.02	13.50	MK-9	0.00	12.52
Q-9	9.47	1.28	MK-10	18.79	1.40
Q-10	0.00	4.14	K_1	0.00	40.61
MK-4	13.90	0.26	PQ-9	0.00	9.66
MK-5	4.84	0.47	TQ[1] (pmol/g)	20.39	10693.66
MK-6	7.49	2.87			

[1]TQ = Total quinones.

> ➢ Quinone indices for characterizing the microbial community

The indices for characterizing the microbial community using the quinone profile are; (a) the types and number of quinone species, (b) dominant quinone species and its molar fraction content, (c) ratio of the total molar fraction contents of ubiquinone (UQ) and menaquinone (MK), (d) diversity of quinone species or divergence index (*MD*), (e) divergence index or dissimilarity (*D*) of quinone profiles, (f) bioenergetic index (*BD*), (g) the total amount of quinones, and so on.

Hedrick and White (1986) demonstrate the value of quinone analysis in ecological studies. Quinone ratios can indicate the redox state for a short-term history (weeks) of oxygen availability in the presence of Gram-negative aerobic, facultative or anaerobic bacteria. The UQ/MK ratio near zero indicates long-term (months) exposure to strictly anaerobic conditions. Values below 1 indicate anaerobic conditions with a past history of oxygen availability (Polglase *et al.*, 1966; Geyer *et al.*, 2004), whereas values around 1 and above indicate an aerobic or microaerophilic environment (anaerobic microniches).

In Ebro delta mat samples the UQ/MK ratio ranged from 1.5–3.0 (Table V.4) that indicated an aerobic or microaerophilic environment at all depths. From 0–0.5 mm the UQ/MK was higher suggesting an important aerophilic character. The values

decreased from 0.5–1.5 mm, and finally the ratio reported higher values at the rest of the vertical profile. At 7–7.75 mm, the ratio slightly decreased indicating a more anaerobic character at the deepest layer. On the other hand, Camargue mat samples showed a wider range of UQ/MK values (0.05–2.5; Table V.5). The uppermost layer of the mat reported a UQ/MK ratio around zero suggesting a more anaerobic character and a predominance of strictly anaerobic bacteria in comparison with the same layer in the Ebro delta mat. Finally, higher values of UQ/MK ratio were detected in the deepest layers of Camargue mats. Apart from that, the 'halophilic pond' and 'Ebro delta all-core' samples reported UQ/MK values of 0.3 and 0.7, respectively suggesting a more anaerobic state in the saltern community (Table V.6).

Ebro delta mats revealed a higher diversity of non-phototrophic microorganisms (*MD* ub+mk value) at 0.5–1 mm and then similar values were reported; whereas in Camargue mat the microbial diversity values were changing with depth and reported the highest diversity of non-phototrophs at the topmost layer and in the deepest part of the mat. The divergence of bioenergetic modes (*BD*) was similar at all depths in the Ebro delta mat, but increased with depth in Camargue mats. Finally, the 'halophilic pond' reported *MD* and *BD* values lower than the 'Ebro delta all-core' sample.

Table V.4. Quinone indices in Ebro Delta microbial mat samples.

Depth (mm)	UQn/MKn	MKn/UQn	*BD* uq+mk	*MD* uq+mk
0–0.5	2.37	0.42	191.39	967.45
0.5–1	1.89	0.53	195.17	1005.12
1–1.5	1.52	0.66	197.87	991.05
1.5–2	2.08	0.48	193.63	927.02
2–2.5	2.46	0.41	190.65	857.92
2.5–3	2.93	0.34	187.11	772.96
3–3.5	2.75	0.36	188.47	747.87
3.5–4	2.18	0.46	192.86	812.33
4–4.5	2.86	0.35	187.63	795.15
4.5–5	2.12	0.47	193.30	857.69
5–5.5	2.78	0.36	188.22	826.97
5.5–6	2.97	0.34	186.85	834.99
6–6.5	2.73	0.37	188.61	874.99
6.5–7	2.17	0.46	192.91	912.38
7–7.75	1.76	0.57	196.13	892.23

Table V.5. Quinone indices in Camargue microbial mat samples.

Depth (mm)	UQn/MKn	MKn/UQn	*BD* uq+mk	*MD* uq+mk
0–0.5	0.18	5.43	172.46	909.55
0.5–1	0.13	7.79	163.51	651.66
1–1.5	0.07	13.75	150.29	580.27
1.5–2	0.05	18.76	143.84	475.69
2–2.5	0.04	26.28	137.58	395.01
2.5–3	0.14	7.40	164.77	674.60
3–3.5	0.13	7.89	163.21	668.19
3.5–4	0.20	5.11	173.99	638.22
4–4.5	0.80	1.25	199.36	874.58
4.5–5	1.02	0.98	200.00	848.53
5–5.5	1.77	0.57	196.08	775.47
5.5–6	2.49	0.40	190.46	724.39
6–6.5	1.30	0.77	199.16	835.99
6.5–7	0.85	1.18	199.65	961.65
7–7.75	0.59	1.70	196.55	893.79

UQ = Ubiquinone; MK = Menaquinone; *MD* ub+mk = Microbial divergence index of ubiquinones and menaquinones; *BD* uq+mk = Bioenergetic divergence index.

Table V.6. Quinone indices in the 'halophilic pond' and 'Ebro delta all- core' samples.

Sample	UQn/MKn	MKn/UQn	*BD* uq+mk	*MD* uq+mk
Halophilic pond	0.26	3.88	180.73	744.17
EBD all core	0.67	1.49	198.07	890.62

In addition, for quantitative assessment of the difference between microbial communities, the dissimilarity (*D*) of quinone profiles can be used (Hiraishi, 1988; Hu *et al.*, 1999). The larger the value of *D*, the more difference between the two quinone profiles. *D* = 0 indicates that the quinone profiles are the same (Hu *et al.*, 2001). In the Ebro delta samples, *D*-values ranged from 3% to 49%, while *D*-values of 4% to 86% were obtained in Camargue samples. Depth related ranges of *D*-values in Ebro delta mat were lower than the difference to Camargue mat and the 'halophilic pond' samples. On the other hand, Camargue's *D*-values were higher in certain depth intervals than in other sampling locations (Table V.7).

A neighbor-joining dendrogram was constructed based on the *D* matrix data (Fig. V.5). Two distinct clusters corresponding to the Ebro delta mat and four clusters corresponding to the Camargue mat were observed. In this case, depth-related differences appeared to have a greater influence than the site-related differences in the structure of microbial communities, which is contrary to results described by Urakawa *et al*. (2005). Indeed, the topmost layers of the Ebro delta mat were clustered together and were closer to the uppermost layers of the Camargue mat than to their deepest layers. Although Ebro delta middle and deepest layers were grouped in the same cluster, were also closely related with Camargue deepest layers, mainly caused by the high content of Q-8 and MK-6 reported in the deepest layers of Camargue mats. In addition, Camargue samples from 4 to 5 mm and from 6 to 7.75 mm (the deepest layers) clustered together with the 'halophilic pond' sample due to the high presence of MK-6, 7 and 8 and Q-8 in both samples. Moreover, the uppermost layers of the Camargue mat were closely related with 'Ebro delta all-core' sample because of their high content in MK-9.

Table V.7. *D*-matrix (EBD Ebro delta 1–15, and CM Camargue 1–15; E: Ebro delta all-core; Hp: Halophilic pond. Decimal positions are omitted.

|	Ebro Delta microbial mat															Camargue microbial mat															E
EBD	1	2	3	4	5	6	7	8	9	10	11	12	13	14	15	1	2	3	4	5	6	7	8	9	10	11	12	13	14	15	E
1																															
2	9																														
3	17	14																													
4	25	22	13																												
5	36	34	27	14																											
6	43	44	39	26	12																										
7	47	49	43	30	16	5																									
8	44	45	37	25	12	8	10																								
9	40	41	33	21	10	11	13	6																							
10	37	36	28	17	9	17	20	11	8																						
11	32	31	23	12	8	16	20	14	10	7																					
12	30	30	25	12	8	16	21	17	14	10	4																				
13	31	30	25	13	7	15	20	16	12	9	6	3																			
14	32	30	22	9	7	17	22	17	14	9	7	6	5																		
15	34	31	21	10	9	20	24	17	14	9	11	11	10	5																	
CM 1	59	54	51	55	58	63	65	58	60	55	60	61	60	57	53																
2	68	65	62	65	66	70	70	63	64	61	66	70	69	67	64	29															
3	73	70	68	71	73	76	76	69	70	67	72	76	75	73	70	37	9														
4	80	78	75	77	77	80	79	73	74	72	77	81	80	78	74	45	16	8													
5	86	83	81	82	83	85	84	79	79	77	82	86	85	83	79	51	22	14	6												
6	68	62	59	61	61	65	66	59	63	58	63	66	65	61	57	28	10	14	20	25											
7	69	63	60	63	62	64	65	58	64	59	65	67	67	63	59	28	11	15	21	26	4										
8	65	60	56	58	58	59	60	53	58	54	60	63	62	58	55	30	14	19	23	29	8	6									
9	45	44	34	27	28	30	29	24	30	25	31	32	31	27	23	45	55	60	66	72	47	47	43								
10	47	46	35	25	22	24	23	18	24	20	24	25	23	19	15	52	63	68	73	78	55	55	51	11							
11	48	46	37	25	15	11	11	13	16	19	18	18	18	17	19	60	69	75	79	84	62	62	58	23	14						
12	46	46	40	27	15	10	11	15	17	19	19	17	16	14	20	61	71	76	81	86	64	65	60	29	21	9					
13	43	41	32	22	18	20	20	18	22	18	19	20	18	14	13	55	67	73	78	83	60	60	56	18	9	13	16				
14	37	36	29	25	26	30	29	25	29	24	29	30	28	24	20	45	57	63	68	74	50	50	46	12	15	23	26	13			
15	44	42	33	35	35	38	37	32	37	32	37	39	37	32	28	42	53	58	63	68	45	45	41	10	14	27	34	21	11		
E	55	52	49	56	63	69	71	70	70	66	66	63	62	61	59	69	69	76	84	89	69	69	67	60	59	61	63	58	55	56	
Hp	43	41	28	29	31	34	34	28	34	28	34	35	34	30	24	47	47	52	57	63	40	40	36	17	22	28	34	24	16	12	58

245
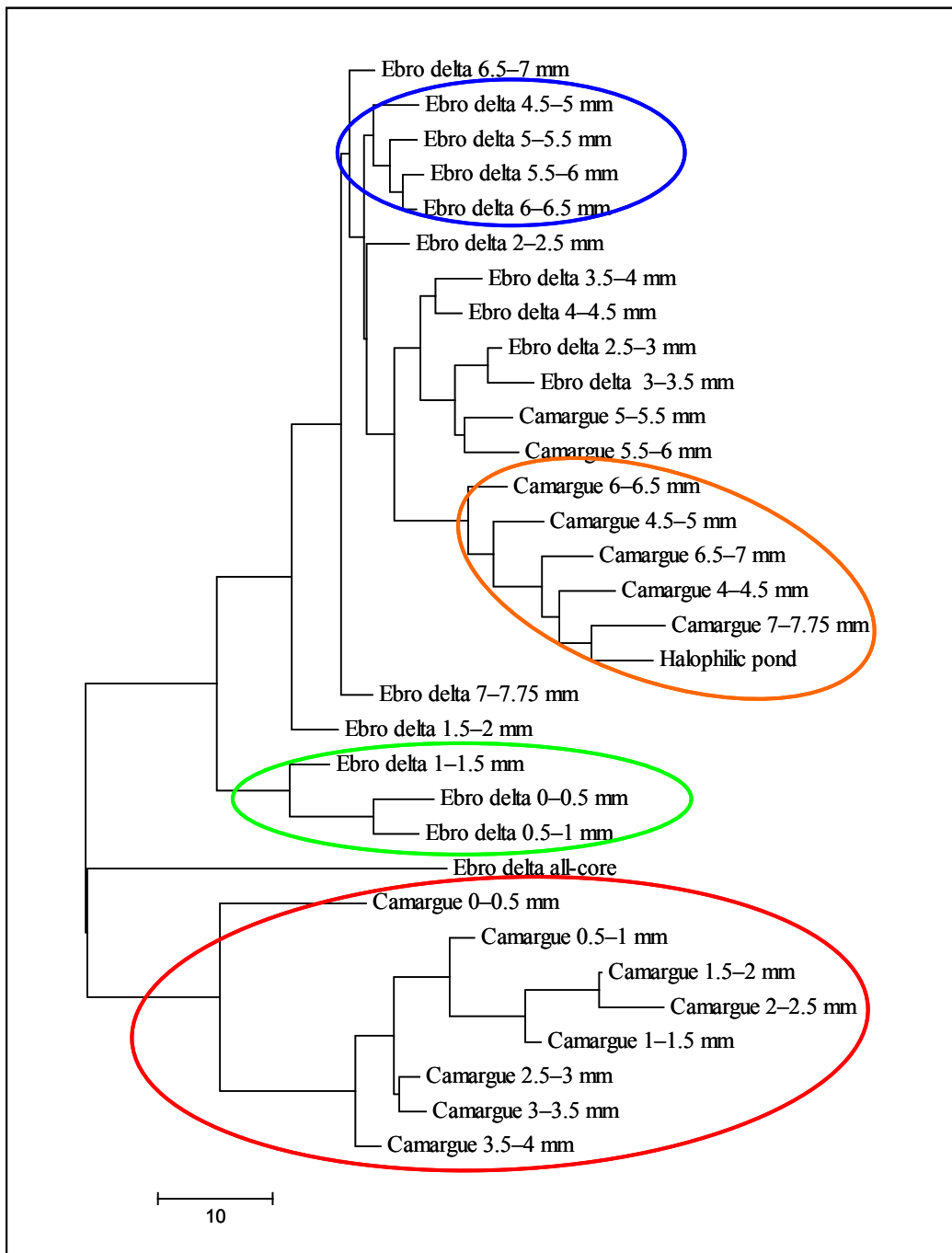
Figure V.5. Neighbor-joining dendrogram describing the dissimilarity (*D*) of quinone profiles deduced from the *D*-value matrix data.

The dendrogram shows the relationships of mat samples. The scale bar indicates a 10% divergence (*D*-value).

➢ Intact polar lipid profiling

Phospholipids were identified based on their mass spectra in the negative ionization mode (Fang and Barcelona, 1998; Murphy, 2002; Pulfer and Murphy, 2003). Structural information of phospholipids was obtained from MS/MS experiments with collisionally induced dissociation (CID) of quasi-molecular ions generated in the electrospray ionization process. The resulting cleavage products revealed the identity of phospholipid type and fatty acid composition. Fragmentation patterns of the detected phospholipids are listed in Table V.8. Positions of fatty acids on the glycerol backbone (*sn* positions) were determined based on the relative intensity of fragment ions representing the fatty acid pair. Fatty acids with the same degree of unsaturation but different position of double bonds were not differentiated.

Several phospholipids were identified in Ebro delta vertical profile samples (Table V.8). The main phospholipids class was phosphatidylglycerol (PG). Moreover, peaks at *m z* 791, 793, 805, 817, 819, 821, 847 and 860 indicated the presence of different sulfoquinovosyldiacylglycerols (SQD) described before as one of the major lipids in cyanobacteria (Murata and Nishida, 1987; Gage *et al.*, 1992; Keusgen *et al.*, 1997). The SQDs were identified by their characteristic fragmentations as previously described by Kim *et al.* (1997). On the *sn*-1 and *sn*-2 positions of the phospholipids were saturated, monounsaturated, and diunsaturated fatty acids with chain lengths from 15 to 19 carbons. The quantification of intact phospholipids was given as counts per seconds (cps) per gram of sample dry weight. The highest amount of phospholipids was found at 2.5–3 mm depth with the exception of C18:0/C18:1-SQD (Fig. V.6 B) that reported maximum values at 3–3.5 mm and C18:0/C18:1-PG that reported important values from 0.5–2.5 mm and decreased thereafter (Fig. V.6 A). In addition, C18:1/C18:1-PG, C16:0/C16:0-PG and C17:0/C15:0-PG followed the same pattern with maximum amounts at 2.5–3 mm, decreased at 3–3.5 mm and finally showed higher values from 3.5 to 4.5 mm depth (Fig. V.6 A). In all cases, the amount of phospholipids was low in the deepest layers and the maximum values were found from 2.5 to 3.5 mm depth. Among phosphatidylglycerols, C18:1/C18:1-PG reached the highest values (4×10^{10} cps per gram of dry weight, Fig. V.6 A) and C16:0/C18:1-SQD was the predominant sulfoquinovosyldiacylglycerol (5.5×10^{10} cps per gram).

Table V.8. Negative molecular ion species [M–H]⁻ assigned in Ebro delta microbial mats.

Polar lipid	*m/z*	FA[1]	FA[2]	Fragment	Rest	Assignation
PG (31:0)	707.6	255.3	241.3	227	211	C16:0/C15:0-PG
PG (32:1)	719.5	255.4	253.4	241, 255 (low)	211	C16:0/C16:1-PG
PG (32:0)	721.6	255.4	255.4	153	211	C16:0/C16:0-PG
PG (32:0)	721.6	269.3	241.3	153	211	C17:0/C15:0-PG
PG (34:2)	745.5	279.3	255.3	153, 171	211	C18:2/C16:0-PG
PG (34:2)	745.5	281.3	253.3	153, 171	211	C18:1/C16:1-PG
PG (34:1)	747.7	281.4	255.4	153, 171	211	C18:1/C16:0-PG
PG (36:2)	773.5	281.3	281.3	153, 171	211	C18:1/C18:1-PG
PG (36:1)	775.6	283.4	281.3	153	211	C18:0/C18:1-PG
PG (37:2)	787.7	281.4	295.6	153, 171	211	C18:1/C19:1-PG
SQD (32:1)	791.7	255.3	253.3	165, 225	283	C16:0/C16:1-SQD
SQD (32:0)	793.7	255.3	255.3	165, 225	283	C16:0/C16:0-SQD
SQD (33:0)	805.5	255.3	253.3	225, 551	297	C16:1/C16:0-SQD-Me[3]
SQD (34:2)	817.6	281.3	253	165, 225	283	C18:1/C16:1 -SQD
SQD (34:1)	819.6	281.3	255.4	165, 225	283	C16:0/C18:1-SQD
SQD (34:0)	821.8	269.3	269.3	165, 225, 241	283	C17:0/C17:0-SQD
SQD (36:1)	847.8	281.3	283.4	113, 227, 241	283	C18:0/C18:1-SQD
SQD (37:1)	860.6	281.3	296.3		283	C18:1/C19:1, *cy*19:0-SQD

[1]FA low abundance *sn*-1 fatty acid; [2]FA high abundance *sn*-2 fatty acid. PG=phosphatidylglycerol, SQD=sulfoquinovosyldiacylglycerol. [3]Assumed methylation at unknown position.
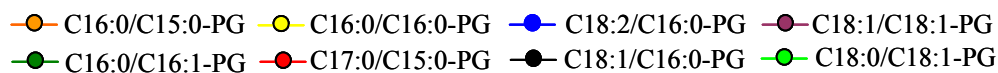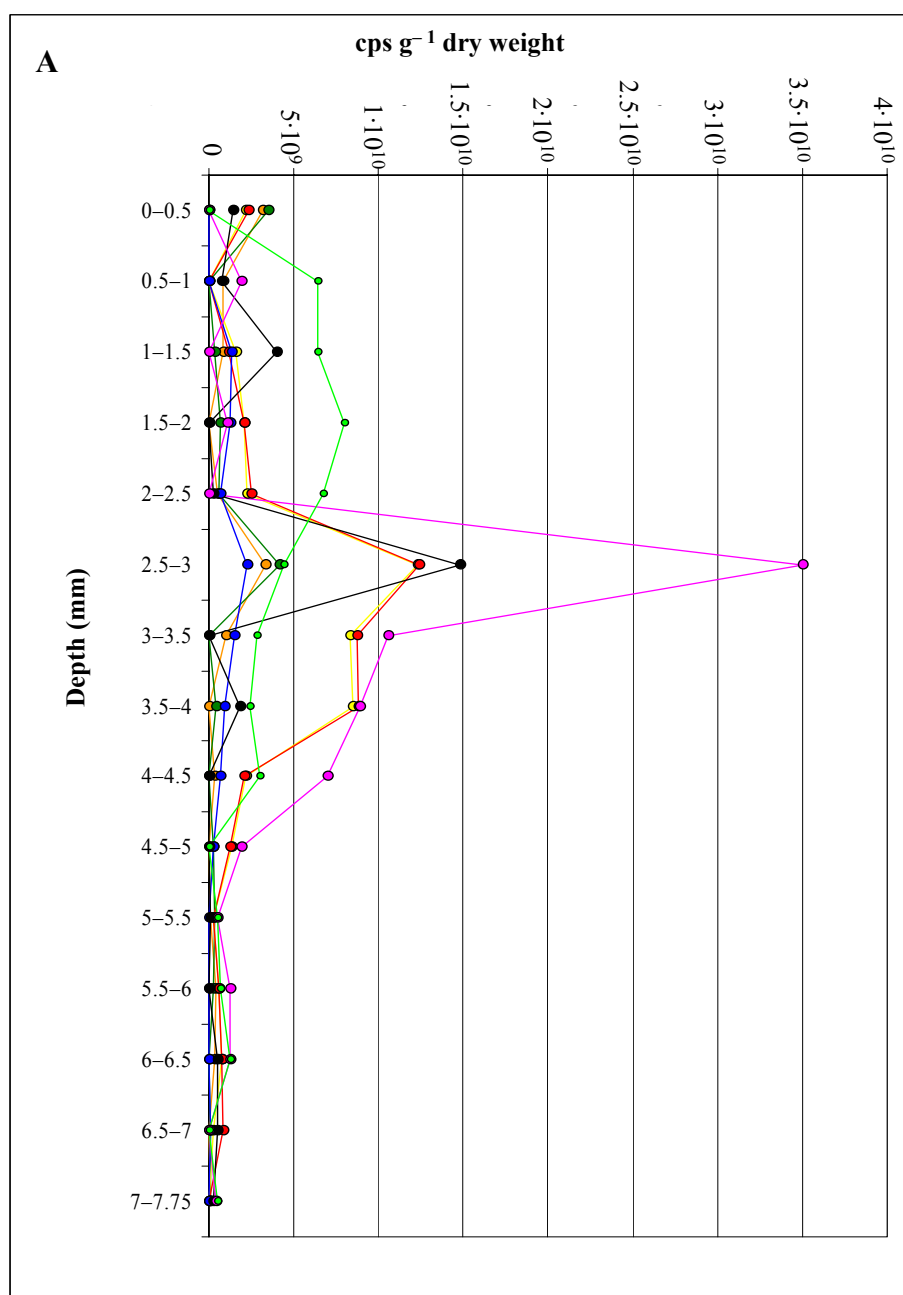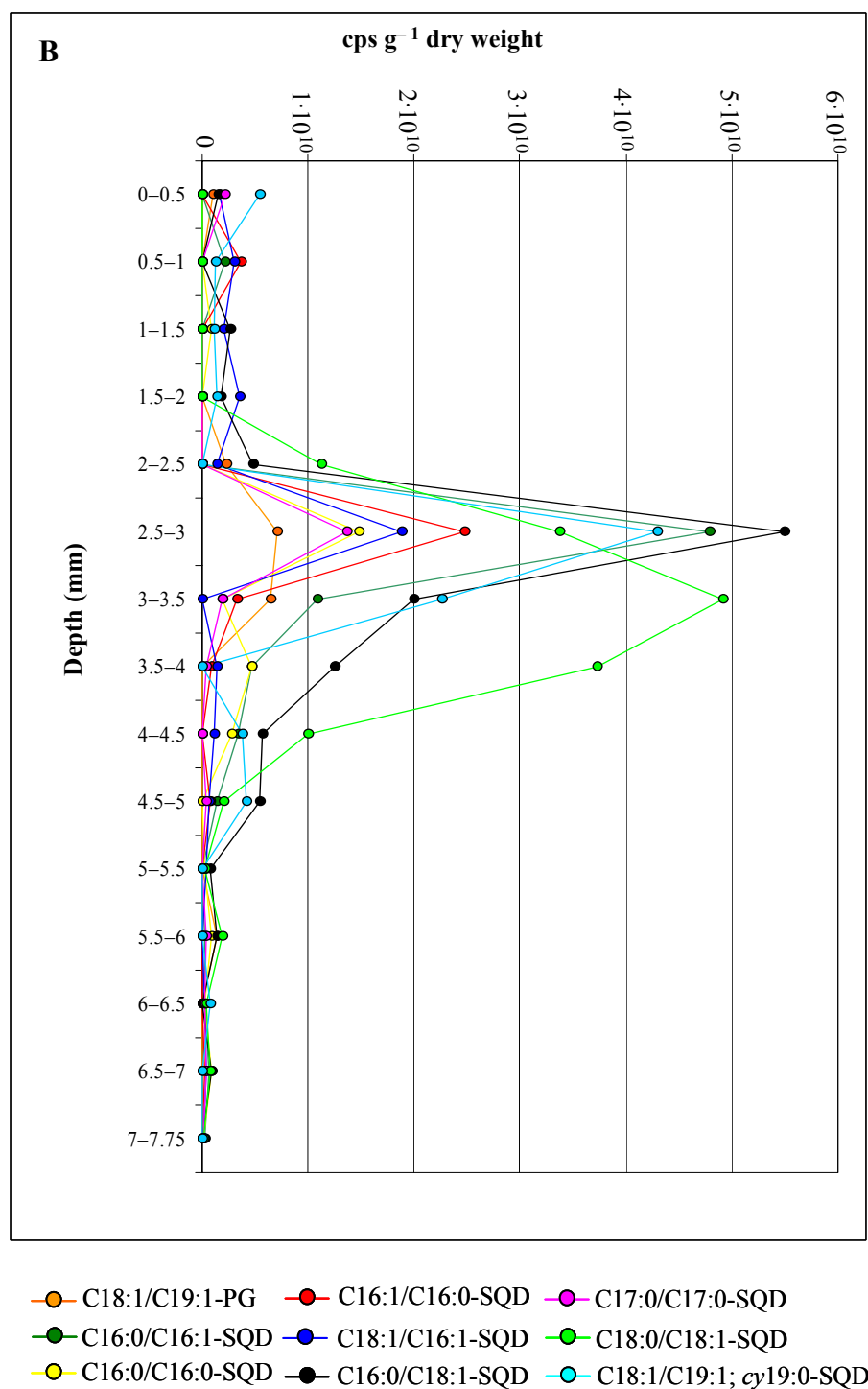
Figure V.6. Vertical distribution of the identified intact phospholipids in Ebro delta mat.

Values given as cps (counts per second; signal response) per gram of dry weight of the sample.

Figure V.6. Vertical distribution of the identified intact phospholipids in Ebro delta mat.

Values given as cps (counts per second; signal response) per gram of dry weight of the sample.

➢ <u>Archaeal sequences in microbial mats</u>

PCR amplification with archaeal primers gave positive signal for the Ebro delta microbial mat sample but failed to amplify archaeal 16S rDNA sequences from total DNA of Camargue mats (extracted from the sample quantity of lyophilized mat sample, 0.15 g). Positive control amplifications with 16S rDNA-universal primers were performed with Camargue-DNA in order to check the optimal conditions of the extracted nucleic acid, and PCR product was obtained.

The archaeal-PCR product from Ebro delta mat sample was cloned in pGEM-T and 37 positive clones were obtained. The sequences inserted in the cloning vector were re-amplified and analyzed by enzyme restrictions. Three different restriction patterns were obtained and two representative clones of each pattern were sequenced. 16S rDNA sequences obtained were only distantly related to those deposited in the database (most within the range 80–90% similarity). The majority of clones were closely related to uncultured *Thermoplasmales* (*Euryarcheota*) and uncultured *Methanomicrobiales* or to other unclassified members of the phylum *Crenarchaeota*. Most of the cloned sequences were not related to any of the known genus (Fig. V.7).
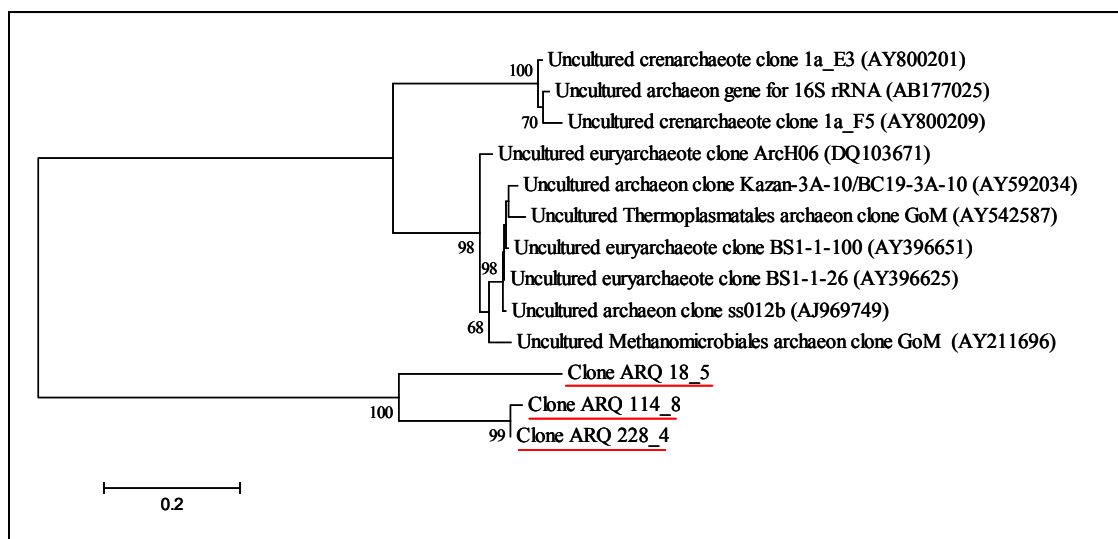

Figure V.7. Phylogenetic tree showing the relationship of the archaeal clones to other archaeal sequences.

The tree was constructed using the Neighbor-joining algorithm (Saitou and Nei, 1987) and the Jukes and Cantor model (Jukes and Cantor, 1966). Numbers on the tree refer to bootstrap values on 1000 replicates. The bar indicates an estimated 20% difference.

- Discussion and conclusions

The application of the quinone profiling approach in Ebro delta and Camargue microbial mats has revealed important differences in the community composition related to sample depth. The higher abundance of Q-8 and Q-10 at all depths in Ebro delta mats suggested a clear predominance of α-, β-, and γ-Proteobacteria (*Rhodobacteraceae*, purple-sulfur bacteria, *Halomonas*, *Beggiatoa*, *Thiomicrospira* sp., and *Alteromonadaceae* most likely). Camargue mats showed a predominance of MK-9 at the top of the mat and Q-8 at the deepest layers, which is consistent with an important contribution of *Firmicutes*, *Actinobacteria* and *Bacteroides* in the photic zone. Moreover, the high %mol of MK-4, -8, and -10 at the topmost layer of Camargue mat also indicated a predominance of members of the phylum *Firmicutes*, *Actinobacteria* and green-non sulfur bacteria (*Chloroflexus*, MK-10). This fact is supported by previous studies performed in Camargue microbial mats (Fourçans *et al*., 2004), in which members of the *Chloroflexus* (MK-10) and *Mycoplasma* (MK-4 as a major quinone) genera have been detected by T-RFLP (terminal restriction fragment length polymorphism). In addition, the importance of members of the *Chloroflexus* genus in Camargue mats has been assessed by DGGE analysis in chapter IV, and it was suggested an important role of *Chloroflexus*-like microorganisms in iron-rich mats (Pierson and Parenteau, 2000). The predominance of menaquinones in Camargue mat samples suggested a predominance of anaerobic bacteria. This fact has been previously related with the higher degree of development and a higher cohesion of Camargue mats in comparison with Ebro delta mats (Navarrete *et al*., 2004) that promote the formation of anaerobic 'microniches'.

Ebro delta mat samples did not show a clear predominance of menaquinones in comparison with Camargue mats with a dominance of MK-9. The high %mol of MK-6 and MK-7 at the top and in the middle layers of the Ebro delta mat indicated a relative importance of members of the *Cytophaga-Flavobacterium* group, *Firmicute*s and δ- and ε-Proteobacteria. Indeed, this data could be related with an unexpected distribution of members of the δ-Proteobacteria (mainly sulfate-reducing bacteria) in the oxic zone of Ebro delta mats as it has been previously proposed by Minz *et al*., 1999, as well as a

higher presence of ε-Proteobacteria, e.g. members of the *Thiomicrospira*, *Arcobacter* genus, etc. (Teske *et al.*, 1996) in Ebro delta mats.

Another important finding was the detection of considerable percentages of photosynthetic quinones, plastoquinone-9 (PQ-9) and phylloquinone (K$_1$) in both systems. These quinones derived from the important population of oxygenic phototrophs (cyanobacteria and diatoms) in layers near the surface of the mat. Although the quantification of photosynthetic quinones was an order of magnitude more in Camargue mats, both microbial systems reported the same pattern of distribution with depth, with the highest amounts between 0.5–2 mm followed by a progressive decrease until a minimum content at approximately 5–6 mm, and finally an increase. This fact supported the idea that more than one functional unit of microbial mat was been analyzed and in this sense the vertical depth from 0–4 mm might correspond to the photosynthetic layer, from 4–7 mm the rest of the mat, and finally starting from 7 mm depth biomarkers from the underlying mat might have remained. This is not surprising because microbial mats form themselves as horizontal layers underlying the previous established mat unit, but this also indicated that the photosynthetic quinones in these kinds of microbial communities have an important resilient time. In fact, this finding can justify future investigations of the degradation rate of quinone homologues in underlying microbial mats units to determine the origin of the photosynthetic quinones.

The quinone composition of the 'halophilic pond' reflected a higher amount of MK-8 as a marker of archaea members (as well as *Firmicutes*, *Acidobacteria*, and δ-Proteobacteria) which is consistent with the important contribution of extremely halophilic *Halobacteriales* in this kind of habitats (Benlloch *et al.*, 2001; Mouné *et al.*, 2003). MK-7 attributed to the halophilic *Bacillus* inhabiting solar salterns (Lim *et al.*, 2005; Yoon *et al.*, 2004 a,b), and Q-8 (mainly members of γ-Proteobacteria such as *Salinimonas, Salinivibrio*, *Halomonas*, *Pseudoalteromonas,* etc.; Jeon *et al.*, 2005; Yeon *et al.*, 2005) were also predominant in this sample, as well as MK-10 attributed to green non-sulfur bacteria. In addition, 'Ebro delta all-core' sample reported a predominance of K$_1$, MK-9 and Q-8. Surprinsingly, the quinone composition of 'Ebro delta vertical-profile' and 'Ebro delta all-core' sample were very different although they were sampled at the same time and site. This divergence can be explained because the

'whole-core' was sampled for lipid analysis purposes and the total depth of the sample was around 2.5 cm, which is around four times deeper compared to the vertical profiles obtained from cryomicrotome cutting of samples (7.75 mm). For this reason, in a whole-core sample many underlying microbial mat units are being analyzed and although they harbour high resilient-time quinones, they will exhibit strong anoxic characteristics and promote the development of anaerobic microbial populations. This fact explains the higher amount of menaquinones, mainly MK-9, as well as the lower UQ/MK ratio in the 'Ebro delta all-core' sample in comparison with the Ebro delta vertical profile.

The redox state index UQ/MK was also different in Ebro delta and Camargue samples indicating a more aerobic or microaerophilic environment in all layers of the Ebro delta mat. Moreover, the 'halophilic pond' and 'Ebro delta all-core' samples reported a low UQ/MK ratio value similar to those observed in the deepest layers of Camargue samples due to the absence of photosynthetic quinones in the 'halophilic pond' sample as well as the higher menaquinone content of both samples. Apart from that, the neighbor-joining dendrogram constructed based on the dissimilarity (*D*) index between samples showed that all samples were strongly influenced by depth-related differences in the structure of the microbial communities.

In correlation with the study of the community composition and the redox state in microbial mat samples by the quinone profiling method, a preliminary study has been performed in order to evaluate the identification and quantification of intact polar lipids in environmental samples. The intact polar lipid (IPL) profiling has been proposed as a complementary approach of the analysis of phopholipid fatty acids (PLFA) because the IPL profiling increases the specificity of the correspondence between polar lipids and microbial groups and improves the characterization of a community (Rütters *et al*., 2002). The more abundant polar lipids expected in the microbial mat systems were those with phosphatidylglycerol (PG) as a polar head group (Ward *et al*., 1994) because PG is the only phospholipid type found in cyanobacteria (Wood, 1988), and phosphatidylethanolamine (PE) which was found to be the dominant phospholipid type in some strains of sulfate-reducing bacteria, Clostridia and also in many other Gram-negative bacteria (Wilkinson, 1988). PG could also derive from a variety of

microorganisms, such as Gram-positive bacteria (O'Leary and Wilkinson, 1988), and Purple-sulfur bacteria (as well as cardiolipin and PE; Imhoff *et al.*, 1982).

A predominance of phosphatidylglycerol polar lipids was detected in Ebro delta mat samples in concordance with previous studies mentioned above. In addition, the most abundant fatty acid combinations in the PGs comprised mainly those fatty acids which also dominate the 'PLFA patterns' after mild alkaline hydrolysis (see results chapter IV) that were C16:0, C16:1, C18:0 and C18:1. Moreover, the detection of several *m z* values that correspond to sulfoquinovosyldiacylglycerols (one of the most important cyanobacterial lipids) and the detection of C18:2 fatty acids (Kenyon, 1972) in the topmost layers of the Ebro delta mat, fit perfectly well with the cyanobacterial distribution in mat systems. Furthermore, C15:0 fatty acids were also detected as components of intact polar lipids as it was previously reported by Rütters *et al.* (1992), and might correspond to sulfate-reducing bacteria (main fatty acids *i*15:0 and *a*15:0). The intact polar lipids were detected until 5 mm depth which also support the reduction of microorganisms and their diversity with increasing depth.

A preliminary detection of archaeal ether lipids has been performed in this study but so far we could not assign the *m/z* values to specific ether lipids. Future studies need to be performed in order to detect the archaeal ether lipids that are supposed to contribute with a higher amount to the total polar lipid content in microbial mats. This fact is supported by a higher quantity of MK-8 and 7 (typical quinones in *Archaea*) in this range of depth. Moreover, archaeal sequences retrieved from Ebro delta microbial mat showed the closest relation to euryarchaeal clones amplified from tidal flat sediments (Kim *et al.*, 2005) related to *Methanomicrobiales* and uncultured *Thermoplasmatales* archaeons. These clones have been detected in diverse locations (Massana *et al.*, 2000; Benlloch *et al.*, 2002), including highly saline deep-sea brines from Kebrit Deep (Eder *et al.*, 1999). The clones affiliated with the phylum *Crenarchaeota* have been detected by sequencing in a wide range of environments and tend to form phylogenetic clusters specific to a given ecosystem (Buckley *et al.*, 1998). Obtained data suggest that the archaeal members of Ebro delta mats might be affiliated with methanogens (*Methanomicrobiales*) but more studies need to be done in order to isolate and characterize the archaeal members in mats. In this sense, if the main archaeal

population in Ebro delta mats belonged to the methanogens a situation of competition for the mineralization of organic carbon to CH_4 would occur between sulfate-reducing bacteria and methanogens (Lovely *et al*., 1982).

In conclusion, the combined use of molecular techniques, and the quinone and intact lipid profiling methods should provide more accurate and reliable quantitative data regarding population dynamics and community structures. Although the universality of quinone profiles as tools for estimating microbial community changes over time and space has been realized, the available information about the quantitative relationships between quinones and microbial biomass is still limited. Moreover, there is also a growing necessity of a more comprehensive database of bacterial IPL profiles. Future studies should be directed at confirming the relationship between abundances of source microorganisms and their lipids biomarkers.

Conclusions

- Community microbial composition and redox state of Ebro delta and Camargue microbial mats have been assessed by structural variations in their quinone profile with depth. The quinone composition has revealed a higher predominance of ubiquinone homologues Q-8 and Q-10 in Ebro delta mats in comparison with Camargue mats, suggesting a dominance of γ- and α-Proteobacteria. Menaquinone-9 was important in Camargue mats which might correspond with a higher presence of *Firmicutes*, *Bacteroides* and *Actinobacteria*, whereas in Ebro delta mats MK-6, 7, and 8 were the most important.

- The detection of photosynthetic quinones (PQ-9 and K_1) indicated that Camargue mats reported a higher biomass of cyanobacteria in comparison with Ebro delta mats.

- The quinone composition of the 'halophilic pond' sample revealed a predominace of archaeal members, halophilic *Bacillus* and γ-Proteobacteria, most likely.

- The index UQ/MK was also different in Ebro delta and Camargue samples indicating a more aerobic or microaerophilic environment in all layers of the Ebro delta mat.

- The dissimilarity (*D*) index showed that the Ebro delta and Camargue vertical-profile samples were more influenced by depth-related differences in the structure of the microbial community than by site-related differences.

- The application of the IPL profiling method revealed a predominance of polar phosphatidylglycerol lipids in Ebro delta mat samples, as well as of fatty acids C16:0, C16:1, C18:0 and C18:1. The detection of the main cyanobacterial lipid sulfoquinovosyldiacylglycerols and C18:2 fatty acids correspond with the cyanobacterial distribution in mat systems.

- Archaeal clones retrieved from Ebro delta mats suggested an affiliation with members of the *Crenarchaeota* and *Euryarcheota* phyla similar to *Thermoplasmatales* and *Methanomicrobiales* sequences.

- **Publications**

- **<u>Villanueva L.</u>, A. Navarrete, J. del Campo, J. Urmeneta, R. Guerrero, and R. Geyer.** Characterization of estuarine microbial mats from different locations by quinone profiling and intact lipid biomarkers. In preparation.